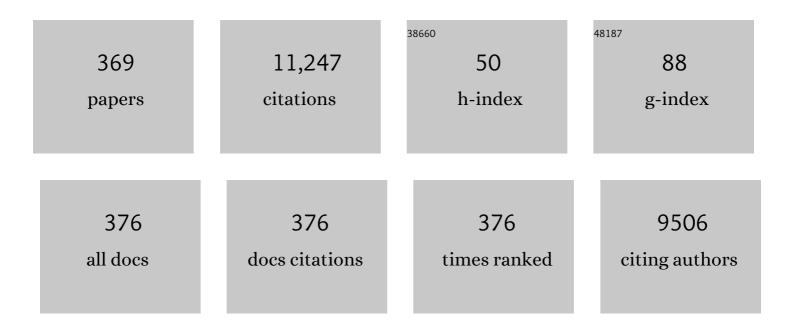
## Yuantong Gu

List of Publications by Year in descending order

Source: https://exaly.com/author-pdf/3722107/publications.pdf Version: 2024-02-01



#	Article	IF	CITATIONS
1	A review of biomass burning: Emissions and impacts on air quality, health and climate in China. Science of the Total Environment, 2017, 579, 1000-1034.	3.9	815
2	A point interpolation method for two-dimensional solids. International Journal for Numerical Methods in Engineering, 2001, 50, 937-951.	1.5	681
3	A LOCAL RADIAL POINT INTERPOLATION METHOD (LRPIM) FOR FREE VIBRATION ANALYSES OF 2-D SOLIDS. Journal of Sound and Vibration, 2001, 246, 29-46.	2.1	461
4	Metalâ€Nitrogenâ€Doped Carbon Materials as Highly Efficient Catalysts: Progress and Rational Design. Advanced Science, 2020, 7, 2001069.	5.6	228
5	Graphene-like Two-Dimensional Ionic Boron with Double Dirac Cones at Ambient Condition. Nano Letters, 2016, 16, 3022-3028.	4.5	222
6	A meshfree radial point interpolation method (RPIM) for three-dimensional solids. Computational Mechanics, 2005, 36, 421-430.	2.2	200
7	A meshless local Petrov-Galerkin (MLPG) method for free and forced vibration analyses for solids. Computational Mechanics, 2001, 27, 188-198.	2.2	165
8	A local point interpolation method for static and dynamic analysis of thin beams. Computer Methods in Applied Mechanics and Engineering, 2001, 190, 5515-5528.	3.4	156
9	Mechanical properties of graphene: Effects of layer number, temperature and isotope. Computational Materials Science, 2013, 71, 197-200.	1.4	146
10	An implicit RBF meshless approach for time fractional diffusion equations. Computational Mechanics, 2011, 48, 1-12.	2.2	142
11	A boundary point interpolation method for stress analysis of solids. Computational Mechanics, 2002, 28, 47-54.	2.2	137
12	Point interpolation method based on local residual formulation using radial basis functions. Structural Engineering and Mechanics, 2002, 14, 713-732.	1.0	116
13	MESHFREE METHODS AND THEIR COMPARISONS. International Journal of Computational Methods, 2005, 02, 477-515.	0.8	113
14	Controllable CO2 electrocatalytic reduction via ferroelectric switching on single atom anchored In2Se3 monolayer. Nature Communications, 2021, 12, 5128.	5.8	110
15	A meshfree method: meshfree weak?strong (MWS) form method, for 2-D solids. Computational Mechanics, 2003, 33, 2-14.	2.2	108
16	Three-dimensional off-design numerical analysis of an organic Rankine cycle radial-inflow turbine. Applied Energy, 2014, 135, 202-211.	5.1	104
17	Meshless local Petrov-Galerkin (MLPG) method in combination with finite element and boundary element approaches. Computational Mechanics, 2000, 26, 536-546.	2.2	98
18	Comparison between the radial point interpolation and the Kriging interpolation used in meshfree methods. Computational Mechanics, 2003, 32, 60-70.	2.2	98

#	Article	IF	CITATIONS
19	A meshless local Kriging method for large deformation analyses. Computer Methods in Applied Mechanics and Engineering, 2007, 196, 1673-1684.	3.4	96
20	Time-dependent fractional advection-diffusion equations by an implicit MLS meshless method. International Journal for Numerical Methods in Engineering, 2011, 88, 1346-1362.	1.5	93
21	Pulmonary aerosol transport and deposition analysis in upper 17 generations of the human respiratory tract. Journal of Aerosol Science, 2017, 108, 29-43.	1.8	89
22	Boundary meshfree methods based on the boundary point interpolation methods. Engineering Analysis With Boundary Elements, 2004, 28, 475-487.	2.0	85
23	From brittle to ductile: a structure dependent ductility of diamond nanothread. Nanoscale, 2016, 8, 11177-11184.	2.8	84
24	Thermal Transport in 3D Nanostructures. Advanced Functional Materials, 2020, 30, 1903841.	7.8	83
25	A point interpolation mesh free method for static and frequency analysis of two-dimensional piezoelectric structures. Computational Mechanics, 2002, 29, 510-519.	2.2	79
26	Assessment and applications of point interpolation methods for computational mechanics. International Journal for Numerical Methods in Engineering, 2004, 59, 1373-1397.	1.5	78
27	Coupling of element free Galerkin and hybrid boundary element methods using modified variational formulation. Computational Mechanics, 2000, 26, 166-173.	2.2	76
28	A coupled element free Galerkin/boundary element method for stress analysis of two-dimensional solids. Computer Methods in Applied Mechanics and Engineering, 2001, 190, 4405-4419.	3.4	76
29	A RBF meshless approach for modeling a fractal mobile/immobile transport model. Applied Mathematics and Computation, 2014, 226, 336-347.	1.4	74
30	Meshless techniques for convection dominated problems. Computational Mechanics, 2006, 38, 171-182.	2.2	73
31	A dynamic wheel–rail impact analysis of railway track under wheel flat by finite element analysis. Vehicle System Dynamics, 2013, 51, 784-797.	2.2	73
32	Thermal conductivity of a new carbon nanotube analog: The diamond nanothread. Carbon, 2016, 98, 232-237.	5.4	71
33	Finite element method for space-time fractional diffusion equation. Numerical Algorithms, 2016, 72, 749-767.	1.1	71
34	Fluid–structure interaction analysis by coupled FE–SPH model based on a novel searching algorithm. Computer Methods in Applied Mechanics and Engineering, 2014, 276, 266-286.	3.4	69
35	A Review of Respiratory Anatomical Development, Air Flow Characterization and Particle Deposition. International Journal of Environmental Research and Public Health, 2020, 17, 380.	1.2	68
36	Scanning Electron Microscopic Study of Microstructure of Gala Apples During Hot Air Drying. Drying Technology, 2014, 32, 455-468.	1.7	67

#	Article	IF	CITATIONS
37	Single Layer Bismuth Iodide: Computational Exploration of Structural, Electrical, Mechanical and Optical Properties. Scientific Reports, 2015, 5, 17558.	1.6	67
38	A radial point interpolation method for simulation of two-dimensional piezoelectric structures. Smart Materials and Structures, 2003, 12, 171-180.	1.8	63
39	Diamond Nanothread as a New Reinforcement for Nanocomposites. Advanced Functional Materials, 2016, 26, 5279-5283.	7.8	63
40	ls the SARS CoV-2 Omicron Variant Deadlier and More Transmissible Than Delta Variant?. International Journal of Environmental Research and Public Health, 2022, 19, 4586.	1.2	63
41	Finite volume and finite element methods for solving a one-dimensional space-fractional Boussinesq equation. Applied Mathematical Modelling, 2014, 38, 3860-3870.	2.2	62
42	The best features of diamond nanothread for nanofibre applications. Nature Communications, 2017, 8, 14863.	5.8	62
43	Graphene and Carbon Nanotube Hybrid Structure: A Review. Procedia IUTAM, 2017, 21, 94-101.	1.2	61
44	Simplest MOF Units for Effective Photodriven Hydrogen Evolution Reaction. Journal of the American Chemical Society, 2018, 140, 9159-9166.	6.6	59
45	Reversible gas capture using a ferroelectric switch and 2D molecule multiferroics on the In <sub>2</sub> Se <sub>3</sub> monolayer. Journal of Materials Chemistry A, 2020, 8, 7331-7338.	5.2	59
46	An enriched radial point interpolation method (e-RPIM) for analysis of crack tip fields. Engineering Fracture Mechanics, 2011, 78, 175-190.	2.0	58
47	<mml:math xmlns:mml="http://www.w3.org/1998/Math/MathML"&gt;<mml:msub><mml:mi>CoB</mml:mi><mml:mn>6monolayer: A robust two-dimensional ferromagnet. Physical Review B, 2019, 99, .</mml:mn></mml:msub></mml:math 	ո <b>։։։ու</b> թե/mr	nl:n5sub>
48	A meshfree weak-strong (MWS) form method for time dependent problems. Computational Mechanics, 2005, 35, 134-145.	2.2	57
49	Comparison of the effectiveness of analytical wake models for wind farm with constant and variable hub heights. Energy Conversion and Management, 2016, 124, 189-202.	4.4	57
50	Distorted Janus Transition Metal Dichalcogenides: Stable Two-Dimensional Materials with Sizable Band Gap and Ultrahigh Carrier Mobility. Journal of Physical Chemistry C, 2018, 122, 19153-19160.	1.5	55
51	A meshless method based on Point Interpolation Method (PIM) for the space fractional diffusion equation. Applied Mathematics and Computation, 2015, 256, 930-938.	1.4	53
52	A coarse-grained red blood cell membrane model to study stomatocyte-discocyte-echinocyte morphologies. PLoS ONE, 2019, 14, e0215447.	1.1	53
53	Comparisons of two meshfree local point interpolation methods for structural analyses. Computational Mechanics, 2002, 29, 107-121.	2.2	52
54	Coupling of the meshfree and finite element methods for determination of the crack tip fields. Engineering Fracture Mechanics, 2008, 75, 986-1004.	2.0	52

Yuantong Gu

#	Article	IF	CITATIONS
55	Modelling of simultaneous heat and mass transfer considering the spatial distribution of air velocity during intermittent microwave convective drying. International Journal of Heat and Mass Transfer, 2020, 153, 119668.	2.5	52
56	Conversion of Catalytically Inert 2D Bismuth Oxide Nanosheets for Effective Electrochemical Hydrogen Evolution Reaction Catalysis via Oxygen Vacancy Concentration Modulation. Nano-Micro Letters, 2022, 14, 90.	14.4	51
57	Predicting a new phase (T′′) of two-dimensional transition metal di-chalcogenides and strain-controlled topological phase transition. Nanoscale, 2016, 8, 4969-4975.	2.8	50
58	Simultaneous removal of cationic and anionic heavy metal contaminants from electroplating effluent by hydrotalcite adsorbent with disulfide ( <mml:math) (xmlns:mml="&lt;/td" 0="" 10="" 50="" 627="" etqq0="" overlock="" rgbt="" td="" tf="" tj=""><td>"http://wv 6.5</td><td>ww.w3.org/19 48</td></mml:math)>	"http://wv 6.5	ww.w3.org/19 48
59	intercalation. Journal of Hazardous Materials, 2020, 382, 121111. Stacking-Dependent Interlayer Magnetic Coupling in 2D Crl <sub>3</sub> /CrGeTe <sub>3</sub> Nanostructures for Spintronics. ACS Applied Nano Materials, 2020, 3, 1282-1288.	2.4	47
60	Application of porous metal foam heat exchangers and the implications of particulate fouling for energy-intensive industries. Chemical Engineering Science, 2020, 228, 115968.	1.9	47
61	Application of Meshless Local Petrov-Galerkin (MLPG) Approach to Simulation of Incompressible Flow. Numerical Heat Transfer, Part B: Fundamentals, 2005, 48, 459-475.	0.6	46
62	AN ADVANCED MESHLESS METHOD FOR TIME FRACTIONAL DIFFUSION EQUATION. International Journal of Computational Methods, 2011, 08, 653-665.	0.8	46
63	Temperature and strain-rate dependent fracture strength of graphynes. Journal Physics D: Applied Physics, 2014, 47, 425301.	1.3	46
64	The morphology and temperature dependent tensile properties of diamond nanothreads. Carbon, 2016, 107, 304-309.	5.4	46
65	High density mechanical energy storage with carbon nanothread bundle. Nature Communications, 2020, 11, 1905.	5.8	45
66	Nanostructured hydroxyapatite surfaces-mediated adsorption alters recognition of BMP receptor IA and bioactivity of bone morphogenetic protein-2. Acta Biomaterialia, 2015, 27, 275-285.	4.1	44
67	Modeling heat transfer during friction stir welding using a meshless particle method. International Journal of Heat and Mass Transfer, 2017, 104, 288-300.	2.5	43
68	A matrix triangularization algorithm for the polynomial point interpolation method. Computer Methods in Applied Mechanics and Engineering, 2003, 192, 2269-2295.	3.4	42
69	Hybrid boundary point interpolation methods and their coupling with the element free Galerkin method. Engineering Analysis With Boundary Elements, 2003, 27, 905-917.	2.0	42
70	Graphene helicoid as novel nanospring. Carbon, 2017, 120, 258-264.	5.4	42
71	Engineering the mechanical properties of CNT/PEEK nanocomposites. RSC Advances, 2019, 9, 12836-12845.	1.7	42
72	Single layer diamond - A new ultrathin 2D carbon nanostructure for mechanical resonator. Carbon, 2020, 161, 809-815.	5.4	42

#	Article	IF	CITATIONS
73	Unsteady natural convection within a differentially heated enclosure of sinusoidal corrugated side walls. International Journal of Heat and Mass Transfer, 2012, 55, 5696-5708.	2.5	40
74	A particle based model to simulate microscale morphological changes of plant tissues during drying. Soft Matter, 2014, 10, 5249-5268.	1.2	40
75	Efficient Removal of Cationic and Anionic Radioactive Pollutants from Water Using Hydrotalcite-Based Getters. ACS Applied Materials & Interfaces, 2016, 8, 16503-16510.	4.0	40
76	Design tools for patient specific and highly controlled melt electrowritten scaffolds. Journal of the Mechanical Behavior of Biomedical Materials, 2020, 105, 103695.	1.5	39
77	A new constraint handling method for wind farm layout optimization with lands owned by different owners. Renewable Energy, 2015, 83, 151-161.	4.3	38
78	Comparative study on optimizing the wind farm layout using different design methods and cost models. Journal of Wind Engineering and Industrial Aerodynamics, 2015, 146, 1-10.	1.7	38
79	Molecular dynamics simulations of adsorption and desorption of bone morphogenetic protein-2 on textured hydroxyapatite surfaces. Acta Biomaterialia, 2018, 80, 121-130.	4.1	38
80	A coupled SPH-DEM model for micro-scale structural deformations of plant cells during drying. Applied Mathematical Modelling, 2014, 38, 3781-3801.	2.2	37
81	A multiscale evaluation of the surface integrity in boring trepanning association deep hole drilling. International Journal of Machine Tools and Manufacture, 2017, 123, 48-56.	6.2	37
82	Two dimensional boron nanosheets: synthesis, properties and applications. Physical Chemistry Chemical Physics, 2018, 20, 28964-28978.	1.3	37
83	Underlying burning resistant mechanisms for titanium alloy. Materials and Design, 2018, 156, 588-595.	3.3	37
84	An extended Galerkin weak form and a point interpolation method with continuous strain field and superconvergence using triangular mesh. Computational Mechanics, 2009, 43, 651-673.	2.2	36
85	A fundamental numerical and theoretical study for the vibrational properties of nanowires. Journal of Applied Physics, 2012, 111, 124303.	1.1	36
86	Numerical investigation of the temporal evolution of particulate fouling in metal foams for air-cooled heat exchangers. Applied Energy, 2016, 184, 531-547.	5.1	36
87	Structure-mediated thermal transport of monolayer graphene allotropes nanoribbons. Carbon, 2014, 77, 416-423.	5.4	35
88	Numerical exploration of plastic deformation mechanisms of copper nanowires with surface defects. Computational Materials Science, 2011, 50, 3425-3430.	1.4	34
89	Beat phenomena in metal nanowires, and their implications for resonance-based elastic property measurements. Nanoscale, 2012, 4, 6779.	2.8	34
90	Ultrafine particle transport and deposition in a large scale 17-generation lung model. Journal of Biomechanics, 2017, 64, 16-25.	0.9	34

Yuantong Gu

#	Article	IF	CITATIONS
91	Accurate Multi-Physics Numerical Analysis of Particle Preconcentration Based on Ion Concentration Polarization. International Journal of Applied Mechanics, 2017, 09, 1750107.	1.3	34
92	A new data-driven topology optimization framework for structural optimization. Computers and Structures, 2020, 239, 106310.	2.4	34
93	Theoretical and numerical investigation of bending properties of Cu nanowires. Computational Materials Science, 2012, 55, 73-80.	1.4	33
94	Facilitated receptor-recognition and enhanced bioactivity of bone morphogenetic protein-2 on magnesium-substituted hydroxyapatite surface. Scientific Reports, 2016, 6, 24323.	1.6	33
95	Impact of Nanoparticle Uptake on the Biophysical Properties of Cell for Biomedical Engineering Applications. Scientific Reports, 2019, 9, 5859.	1.6	33
96	Effect of Reynolds numbers on flow past four square cylinders in an in-line square configuration for different gap spacings. Journal of Mechanical Science and Technology, 2014, 28, 539-552.	0.7	32
97	Euler-Lagrange Prediction of Diesel-Exhaust Polydisperse Particle Transport and Deposition in Lung: Anatomy and Turbulence Effects. Scientific Reports, 2019, 9, 12423.	1.6	32
98	Optical coherence tomography-based patient-specific coronary artery reconstruction and fluid–structure interaction simulation. Biomechanics and Modeling in Mechanobiology, 2020, 19, 7-20.	1.4	32
99	SARS CoV-2 aerosol: How far it can travel to the lower airways?. Physics of Fluids, 2021, 33, 061903.	1.6	32
100	Graphene ripples generated by grain boundaries in highly ordered pyrolytic graphite. Carbon, 2014, 68, 330-336.	5.4	31
101	Investigation of red blood cell mechanical properties using AFM indentation and coarse-grained particle method. BioMedical Engineering OnLine, 2017, 16, 140.	1.3	31
102	Suppressed Thermal Conductivity of Bilayer Graphene with Vacancy-Initiated Linkages. Journal of Physical Chemistry C, 2015, 119, 1748-1752.	1.5	30
103	Failure mechanism of monolayer graphene under hypervelocity impact of spherical projectile. Scientific Reports, 2016, 6, 33139.	1.6	30
104	Neutral and charged boron-doped fullerenes for CO <sub>2</sub> adsorption. Beilstein Journal of Nanotechnology, 2014, 5, 413-418.	1.5	29
105	Application of meshfree methods to numerically simulate microscale deformations of different plant food materials during drying. Journal of Food Engineering, 2015, 146, 209-226.	2.7	29
106	Polydisperse Microparticle Transport and Deposition to the Terminal Bronchioles in a Heterogeneous Vasculature Tree. Scientific Reports, 2018, 8, 16387.	1.6	29
107	Biophysical response of living cells to boron nitride nanoparticles: uptake mechanism and bio-mechanical characterization. Journal of Nanoparticle Research, 2015, 17, 1.	0.8	28
108	Mechanical Properties of Penta-Graphene Nanotubes. Journal of Physical Chemistry C, 2017, 121, 9642-9647.	1.5	28

#	Article	IF	CITATIONS
109	Optimization of wind farm layout with complex land divisions. Renewable Energy, 2017, 105, 30-40.	4.3	28
110	Reproducing kernel particle method for two-dimensional time-space fractional diffusion equations in irregular domains. Engineering Analysis With Boundary Elements, 2018, 97, 131-143.	2.0	28
111	Polydisperse Aerosol Transport and Deposition in Upper Airways of Age-Specific Lung. International Journal of Environmental Research and Public Health, 2021, 18, 6239.	1.2	28
112	Machine learningâ€based modeling in food processing applications: State of the art. Comprehensive Reviews in Food Science and Food Safety, 2022, 21, 1409-1438.	5.9	28
113	Tensile properties of a boron/nitrogen-doped carbon nanotube–graphene hybrid structure. Beilstein Journal of Nanotechnology, 2014, 5, 329-336.	1.5	27
114	A novel control strategy approach to optimally design a wind farm layout. Renewable Energy, 2016, 95, 10-21.	4.3	27
115	Analysis of particle-laden fluid flows, tortuosity and particle-fluid behaviour in metal foam heat exchangers. Chemical Engineering Science, 2017, 172, 677-687.	1.9	27
116	Novel trends in numerical modelling of plant food tissues and their morphological changes during drying – A review. Journal of Food Engineering, 2017, 194, 24-39.	2.7	27
117	Breakdown of Hooke's law at the nanoscale – 2D material-based nanosprings. Nanoscale, 2018, 10, 18961-18968.	2.8	27
118	Modeling of mass transfer enhancement in a magnetofluidic micromixer. Physics of Fluids, 2019, 31, .	1.6	27
119	Tuning Magnetism of Metal Porphyrazine Molecules by a Ferroelectric In <sub>2</sub> Se <sub>3</sub> Monolayer. ACS Applied Materials & Interfaces, 2020, 12, 39561-39566.	4.0	27
120	Low interfacial thermal resistance between crossed ultra-thin carbon nanothreads. Carbon, 2020, 165, 216-224.	5.4	27
121	Thermal conductivity of configurable two-dimensional carbon nanotube architecture and strain modulation. Applied Physics Letters, 2014, 105, .	1.5	26
122	Effectiveness of optimized control strategy and different hub height turbines on a real wind farm optimization. Renewable Energy, 2018, 126, 819-829.	4.3	26
123	How severe acute respiratory syndrome coronavirus-2 aerosol propagates through the age-specific upper airways. Physics of Fluids, 2021, 33, 081911.	1.6	26
124	Investigation of Cell-Substrate Adhesion Properties of Living Chondrocyte by Measuring Adhesive Shear Force and Detachment Using AFM and Inverse FEA. Scientific Reports, 2016, 6, 38059.	1.6	25
125	Graphene Helicoid: Distinct Properties Promote Application of Graphene Related Materials in Thermal Management. Journal of Physical Chemistry C, 2018, 122, 7605-7612.	1.5	25
126	2D ferroelectric devices: working principles and research progress. Physical Chemistry Chemical Physics, 2021, 23, 21376-21384.	1.3	25

#	Article	IF	CITATIONS
127	The stress-strain relationship of liquid marbles under compression. Applied Physics Letters, 2019, 114, 043701.	1.5	24
128	Interaction of gold nanosurfaces/nanoparticles with collagen-like peptides. Physical Chemistry Chemical Physics, 2019, 21, 3701-3711.	1.3	24
129	Multiferroic decorated Fe <sub>2</sub> O <sub>3</sub> monolayer predicted from first principles. Nanoscale, 2020, 12, 14847-14852.	2.8	24
130	Simulation of plant cell shrinkage during drying – A SPH–DEM approach. Engineering Analysis With Boundary Elements, 2014, 44, 1-18.	2.0	23
131	Numerical investigation of plant tissue porosity and its influence on cellular level shrinkage during drying. Biosystems Engineering, 2015, 132, 71-87.	1.9	23
132	An advanced numerical modeling for Riesz space fractional advection–dispersion equations by a meshfree approach. Applied Mathematical Modelling, 2016, 40, 7816-7829.	2.2	23
133	Strained graphitic carbon nitride for hydrogen purification. Journal of Membrane Science, 2017, 528, 201-205.	4.1	23
134	A computationally-efficient layout optimization method for real wind farms considering altitude variations. Energy, 2017, 132, 147-159.	4.5	23
135	A Concurrent Multiscale Method Based on the Meshfree Method and Molecular Dynamics Analysis. Multiscale Modeling and Simulation, 2006, 5, 1128-1155.	0.6	22
136	Design methods of rhombic tensegrity structures. Acta Mechanica Sinica/Lixue Xuebao, 2010, 26, 559-565.	1.5	22
137	A HYBRID SMOOTHED FINITE ELEMENT METHOD (H-SFEM) TO SOLID MECHANICS PROBLEMS. International Journal of Computational Methods, 2013, 10, 1340011.	0.8	22
138	Thermal conductivity of Si nanowires with faulted stacking layers. Journal Physics D: Applied Physics, 2014, 47, 015303.	1.3	22
139	Natural convection in a triangular enclosure heated from below and non-uniformly cooled from top. International Journal of Heat and Mass Transfer, 2015, 80, 529-538.	2.5	22
140	Meshless methods coupled with other numerical methods. Tsinghua Science and Technology, 2005, 10, 8-15.	4.1	21
141	Hierarchical multiscale model for biomechanics analysis of microfilament networks. Journal of Applied Physics, 2013, 113, 194701.	1.1	21
142	Acoustic analysis using a mass-redistributed smoothed finite element method with quadrilateral mesh. Engineering Computations, 2015, 32, 2292-2317.	0.7	21
143	A three-dimensional hybrid smoothed finite element method (H-SFEM) for nonlinear solid mechanics problems. Acta Mechanica, 2015, 226, 4223-4245.	1.1	21
144	Theoretical investigation of calcium-decorated β12 boron sheet for hydrogen storage. Chemical Physics Letters, 2018, 695, 211-215.	1.2	21

#	Article	IF	CITATIONS
145	Development of realistic food microstructure considering the structural heterogeneity of cells and intercellular space. Food Structure, 2018, 15, 9-16.	2.3	21
146	Characterisation on the hygrothermal degradation in the mechanical property of structural adhesive: A novel meso-scale approach. Composites Part B: Engineering, 2020, 182, 107609.	5.9	21
147	Modified beam theories for bending properties of nanowires considering surface/intrinsic effects and axial extension effect. Journal of Applied Physics, 2012, 111, .	1.1	20
148	Heterogeneous nanomechanical properties of type I collagen in longitudinal direction. Biomechanics and Modeling in Mechanobiology, 2017, 16, 1023-1033.	1.4	20
149	Notch expressed by osteocytes plays a critical role in mineralisation. Journal of Molecular Medicine, 2018, 96, 333-347.	1.7	20
150	Steered molecular dynamics characterization of the elastic modulus and deformation mechanisms of single natural tropocollagen molecules. Journal of the Mechanical Behavior of Biomedical Materials, 2018, 86, 359-367.	1.5	20
151	Aberrant activation of Wnt signaling pathway altered osteocyte mineralization. Bone, 2019, 127, 324-333.	1.4	20
152	Adsorption of Collagen-like Peptides onto Gold Nanosurfaces. Langmuir, 2019, 35, 4435-4444.	1.6	20
153	Development of Mechanically Enhanced Polycaprolactone Composites by a Functionalized Titanate Nanofiller for Melt Electrowriting in 3D Printing. ACS Applied Materials & Interfaces, 2020, 12, 47993-48006.	4.0	20
154	Hydrogen-Intercalated 2D Magnetic Bilayer: Controlled Magnetic Phase Transition and Half-Metallicity via Ferroelectric Switching. ACS Applied Materials & Interfaces, 2022, 14, 1800-1806.	4.0	20
155	A coupled finite volume & discrete element method to examine particulate foulant transport in metal foam heat exchangers. International Journal of Heat and Mass Transfer, 2017, 115, 43-61.	2.5	19
156	A new regularization method for the dynamic load identification of stochastic structures. Computers and Mathematics With Applications, 2018, 76, 741-759.	1.4	19
157	Numerical Study of Impact Forces on Railway Sleepers under Wheel Flat. Advances in Structural Engineering, 2013, 16, 127-134.	1.2	18
158	Exploration of mechanisms underlying the strain-rate-dependent mechanical property of single chondrocytes. Applied Physics Letters, 2014, 104, 183701.	1.5	18
159	Mechanical bending properties of sodium titanate (Na <sub>2</sub> Ti <sub>3</sub> O <sub>7</sub> ) nanowires. RSC Advances, 2014, 4, 56970-56976.	1.7	18
160	Numerical Investigation of Case Hardening of Plant Tissue During Drying and Its Influence on the Cellular-Level Shrinkage. Drying Technology, 2015, 33, 713-734.	1.7	18
161	Substantial Band-Gap Tuning and a Strain-Controlled Semiconductor to Gapless/Band-Inverted Semimetal Transition in Rutile Lead/Stannic Dioxide. ACS Applied Materials & Interfaces, 2016, 8, 25667-25673.	4.0	18
162	SPH-DEM approach to numerically simulate the deformation of three-dimensional RBCs in non-uniform capillaries. BioMedical Engineering OnLine, 2016, 15, 161.	1.3	18

#	Article	IF	CITATIONS
163	A Comparative Study of Mixed Resolved–Unresolved CFD-DEM and Unresolved CFD-DEM Methods for the Solution of Particle-Laden Liquid Flows. Archives of Computational Methods in Engineering, 2019, 26, 1239-1254.	6.0	18
164	A general Neural Particle Method for hydrodynamics modeling. Computer Methods in Applied Mechanics and Engineering, 2022, 393, 114740.	3.4	18
165	Surface effects on the dual-mode vibration of 〈1 1 0〉 silver nanowires with different cross-section Journal Physics D: Applied Physics, 2012, 45, 465304.	<sup>1S.</sup> 1.3	17
166	Bending properties of Ag nanowires with pre-existing surface defects. Computational Materials Science, 2014, 81, 45-51.	1.4	17
167	Control of flow around a circular cylinder wrapped with a porous layer by magnetohydrodynamic. Journal of Magnetism and Magnetic Materials, 2016, 401, 1078-1087.	1.0	17
168	Impact and energy absorption of portable water-filled road safety barrier system fitted with foam. International Journal of Impact Engineering, 2014, 72, 26-39.	2.4	16
169	Molecular insights on the interference of simplified lung surfactant models by gold nanoparticle pollutants. Biochimica Et Biophysica Acta - Biomembranes, 2019, 1861, 1458-1467.	1.4	16
170	Steady Natural Convection of Non-Newtonian Power-Law Fluid in a Trapezoidal Enclosure. Advances in Mechanical Engineering, 2013, 5, 653108.	0.8	16
171	Analysis of microelectromechanical systems (mems) by meshless local kriging (lokriging) method. Journal of the Chinese Institute of Engineers, Transactions of the Chinese Institute of Engineers,Series A/Chung-kuo Kung Ch'eng Hsuch K'an, 2004, 27, 573-583.	0.6	15
172	Mechanical properties of bioinspired bicontinuous nanocomposites. Computational Materials Science, 2013, 80, 71-78.	1.4	15
173	Determination of Strain-Rate-Dependent Mechanical Behavior of Living and Fixed Osteocytes and Chondrocytes Using Atomic Force Microscopy and Inverse Finite Element Analysis. Journal of Biomechanical Engineering, 2014, 136, 101004.	0.6	15
174	Turbulent dense gas flow characteristics in swirling conical diffuser. Computers and Fluids, 2017, 149, 100-118.	1.3	15
175	Coupled CFD-DEM simulation of oscillatory particle-laden fluid flow through a porous metal foam heat exchanger: Mitigation of particulate fouling. Chemical Engineering Science, 2018, 179, 32-52.	1.9	15
176	<i>In situ</i> mechanical resonance behaviour of pristine and defective zinc blende GaAs nanowires. Nanoscale, 2018, 10, 2588-2595.	2.8	15
177	<i>In Situ</i> Atomic-Scale Study on the Ultralarge Bending Behaviors of TiO <sub>2</sub> –B/Anatase Dual-Phase Nanowires. Nano Letters, 2019, 19, 7742-7749.	4.5	15
178	Chitosan/graphene complex membrane for polymer electrolyte membrane fuel cell: A molecular dynamics simulation study. International Journal of Hydrogen Energy, 2020, 45, 25960-25969.	3.8	15
179	Robust Magnetoelectric Effect in the Decorated Graphene/In <sub>2</sub> Se <sub>3</sub> Heterostructure. ACS Applied Materials & Interfaces, 2021, 13, 3033-3039.	4.0	15
180	3D Printed Multi-Functional Scaffolds Based on Poly(Îμ-Caprolactone) and Hydroxyapatite Composites. Nanomaterials, 2021, 11, 2456.	1.9	15

#	Article	IF	CITATIONS
181	Advanced Numerical Characterization of Mono-Crystalline Copper with Defects. Advanced Science Letters, 2011, 4, 1293-1301.	0.2	15
182	A new tip area function for instrumented nanoindentation at extremely small contact depths. Materials Science & Engineering A: Structural Materials: Properties, Microstructure and Processing, 2011, 528, 7948-7951.	2.6	14
183	Deconvolution of mechanical properties of thin films from nanoindentation measurement via finite element optimization. Thin Solid Films, 2012, 526, 183-190.	0.8	14
184	Adhesive characteristics of low dimensional carbon nanomaterial on actin. Applied Physics Letters, 2014, 104, .	1.5	14
185	Molecular investigation of the mechanical properties of single actin filaments based on vibration analyses. Computer Methods in Biomechanics and Biomedical Engineering, 2014, 17, 616-622.	0.9	14
186	Fluid–structure interaction analysis of full scale vehicle-barrier impact using coupled SPH–FEA. Engineering Analysis With Boundary Elements, 2014, 42, 26-36.	2.0	14
187	Tailoring the Resonance of Bilayer Graphene Sheets by Interlayer sp <sup>3</sup> Bonds. Journal of Physical Chemistry C, 2014, 118, 732-739.	1.5	14
188	Natural convection due to differential heating of inclined walls and heat source placed on bottom wall of an attic shaped space. Energy and Buildings, 2015, 89, 153-162.	3.1	14
189	High-mobility anisotropic transport in few-layer γ-B <sub>28</sub> films. Nanoscale, 2016, 8, 20111-20117.	2.8	14
190	Investigation of the Effects of Extracellular Osmotic Pressure on Morphology and Mechanical Properties of Individual Chondrocyte. Cell Biochemistry and Biophysics, 2016, 74, 229-240.	0.9	14
191	Thermal conduction of one-dimensional carbon nanomaterials and nanoarchitectures. Chinese Physics B, 2018, 27, 038103.	0.7	14
192	Numerical investigation of atherosclerotic plaque rupture using optical coherence tomography imaging and XFEM. Engineering Fracture Mechanics, 2018, 204, 531-541.	2.0	14
193	Single-molecule insights into surface-mediated homochirality in hierarchical peptide assembly. Nature Communications, 2018, 9, 2711.	5.8	14
194	A novel super-elastic carbon nanofiber with cup-stacked carbon nanocones and a screw dislocation. Carbon, 2019, 154, 98-107.	5.4	14
195	A coarse-grained multiscale model to simulate morphological changes of food-plant tissues undergoing drying. Soft Matter, 2019, 15, 901-916.	1.2	14
196	Modelling of Red Blood Cell Morphological and Deformability Changes during In-Vitro Storage. Applied Sciences (Switzerland), 2020, 10, 3209.	1.3	14
197	Helium–Oxygen Mixture Model for Particle Transport in CT-Based Upper Airways. International Journal of Environmental Research and Public Health, 2020, 17, 3574.	1.2	14
198	Anomalous sub-diffusion equations by the meshless collocation method. Australian Journal of Mechanical Engineering, 2012, 10, 1-8.	1.5	13

#	Article	IF	CITATIONS
199	Two-dimensional graphene heterojunctions: The tunable mechanical properties. Carbon, 2015, 95, 1061-1068.	5.4	13
200	Role of Nitrogen on the Mechanical Properties of the Novel Carbon Nitride Nanothreads. Journal of Physical Chemistry C, 2019, 123, 28977-28984.	1.5	13
201	Carotid Bifurcation With Tandem Stenosis—A Patient-Specific Case Study Combined in vivo Imaging, in vitro Histology and in silico Simulation. Frontiers in Bioengineering and Biotechnology, 2019, 7, 349.	2.0	13
202	Transient heat transfer and non-isothermal particle-laden gas flows through porous metal foams of differing structure. Applied Thermal Engineering, 2019, 150, 888-903.	3.0	13
203	High efficient arsenic removal by In-layer sulphur of layered double hydroxide. Journal of Colloid and Interface Science, 2022, 608, 2358-2366.	5.0	13
204	A pseudo-elastic local meshless method for analysis of material nonlinear problems in solids. Engineering Analysis With Boundary Elements, 2007, 31, 771-782.	2.0	12
205	Scaling for the Prandtl number of the natural convection boundary layer of an inclined flat plate under uniform surface heat flux. International Journal of Heat and Mass Transfer, 2012, 55, 2394-2401.	2.5	12
206	Graphene with Patterned Fluorination: Morphology Modulation and Implications. Journal of Physical Chemistry C, 2015, 119, 27562-27568.	1.5	12
207	A poroviscohyperelastic model for numerical analysis of mechanical behavior of single chondrocyte. Computer Methods in Biomechanics and Biomedical Engineering, 2016, 19, 126-136.	0.9	12
208	Polypeptide-rhodamine B probes containing laminin/fibronectin receptor-targeting sequence (YIGSR/RGD) for fluorescent imaging in cancers. Talanta, 2020, 212, 120718.	2.9	12
209	Molecular Dynamics Simulation of Chiral Carbon Nanothread Bundles for Nanofiber Applications. ACS Applied Nano Materials, 2020, 3, 10218-10225.	2.4	12
210	A CONFORMING POINT INTERPOLATION METHOD (CPIM) BY SHAPE FUNCTION RECONSTRUCTION FOR ELASTICITY PROBLEMS. International Journal of Computational Methods, 2010, 07, 369-395.	0.8	11
211	Heat Transfer Analysis of Viscous Incompressible Fluid by Combined Natural Convection and Radiation in an Open Cavity. Mathematical Problems in Engineering, 2014, 2014, 1-14.	0.6	11
212	Transient air flow and heat transfer in a triangular enclosure with a conducting partition. Applied Mathematical Modelling, 2014, 38, 3879-3887.	2.2	11
213	Microscale consolidation analysis of relaxation behavior of single living chondrocytes subjected to varying strain-rates. Journal of the Mechanical Behavior of Biomedical Materials, 2015, 49, 343-354.	1.5	11
214	Tailorable Burning Behavior of Ti14 Alloy by Controlling Semi-Solid Forging Temperature. Materials, 2016, 9, 697.	1.3	11
215	First-principles prediction of ferroelasticity tuned anisotropic auxeticity and carrier mobility in two-dimensional AgO. Journal of Materials Chemistry C, 2021, 9, 3155-3160.	2.7	11
216	A point interpolation method with locally smoothed strain field (PIM-LS2) for mechanics problems using triangular mesh. Finite Elements in Analysis and Design, 2010, 46, 862-874.	1.7	10

#	Article	IF	CITATIONS
217	An Enriched Radial Point Interpolation Method Based on Weak-Form and Strong-Form. Mechanics of Advanced Materials and Structures, 2011, 18, 578-584.	1.5	10
218	MD INVESTIGATIONS FOR MECHANICAL PROPERTIES OF COPPER NANOWIRES WITH AND WITHOUT SURFACE DEFECTS. International Journal of Computational Methods, 2012, 09, 1240003.	0.8	10
219	Unsteady Natural Convection Within a Porous Enclosure of Sinusoidal Corrugated Side Walls. Transport in Porous Media, 2014, 104, 537-552.	1.2	10
220	A coupled SPH-DEM approach to model the interactions between multiple red blood cells in motion in capillaries. International Journal of Mechanics and Materials in Design, 2016, 12, 477-494.	1.7	10
221	Application of a coupled smoothed particle hydrodynamics (SPH) and coarse-grained (CG) numerical modelling approach to study three-dimensional (3-D) deformations of single cells of different food-plant materials during drying. Soft Matter, 2018, 14, 2015-2031.	1.2	10
222	Application of 3D imaging and analysis techniques for the study of food plant cellular deformations during drying. Drying Technology, 2018, 36, 509-522.	1.7	10
223	Effect of hydroxylysine-O-glycosylation on the structure of type I collagen molecule: A computational study. Glycobiology, 2020, 30, 830-843.	1.3	10
224	Deformation behaviour of stomatocyte, discocyte and echinocyte red blood cell morphologies during optical tweezers stretching. Biomechanics and Modeling in Mechanobiology, 2020, 19, 1827-1843.	1.4	10
225	Carbon nanothreads enable remarkable enhancement in the thermal conductivity of polyethylene. Nanoscale, 2021, 13, 6934-6943.	2.8	10
226	Phase engineering of dual active 2D Bi <sub>2</sub> O <sub>3</sub> -based nanocatalysts for alkaline hydrogen evolution reaction electrocatalysis. Journal of Materials Chemistry A, 2022, 10, 808-817.	5.2	10
227	Numerical Exploration of the Defect's Effect on Mechanical Properties of Nanowires under Torsion. Advanced Materials Research, 0, 335-336, 498-501.	0.3	9
228	Impact & Energy Absorption of Road Safety Barriers by Coupled SPH/FEM. International Journal of Protective Structures, 2012, 3, 257-273.	1.4	9
229	TENSILE PROPERTIES OF GRAPHENE-NANOTUBE HYBRID STRUCTURES: A MOLECULAR DYNAMICS STUDY. International Journal of Computational Materials Science and Engineering, 2013, 02, 1350020.	0.5	9
230	Similarity Solutions for Flow and Heat Transfer of Non-Newtonian Fluid over a Stretching Surface. Journal of Applied Mathematics, 2014, 2014, 1-8.	0.4	9
231	Carbon nanotube-based super nanotubes: tunable thermal conductivity in three dimensions. RSC Advances, 2015, 5, 48164-48168.	1.7	9
232	Interaction pressure tensor on high-order lattice Boltzmann models for nonideal fluids. Physical Review E, 2019, 99, 063318.	0.8	9
233	Effective Enhancement of a Carbon Nanothread on the Mechanical Properties of the Polyethylene Nanocomposite. Journal of Physical Chemistry C, 2021, 125, 5781-5792.	1.5	9
234	A bio-inspired B-Spline Offset Feature for structural topology optimization. Computer Methods in Applied Mechanics and Engineering, 2021, 386, 114081.	3.4	9

#	Article	IF	CITATIONS
235	Stress relaxation analysis of single chondrocytes using porohyperelastic model based on AFM experiments. Theoretical and Applied Mechanics Letters, 2014, 4, 054001.	1.3	8
236	A sub‒domain smoothed Galerkin method for solid mechanics problems. International Journal for Numerical Methods in Engineering, 2014, 98, 781-798.	1.5	8
237	Effect of joint mechanism on vehicle redirectional capability of water-filled road safety barrier systems. Accident Analysis and Prevention, 2014, 71, 60-71.	3.0	8
238	Variable-based Ramberg–Osgood constitutive model of power spinning bushing. Transactions of Nonferrous Metals Society of China, 2015, 25, 3080-3087.	1.7	8
239	Effects of surface atomistic modification on mechanical properties of gold nanowires. Physics Letters, Section A: General, Atomic and Solid State Physics, 2015, 379, 1893-1897.	0.9	8
240	Adaptive finite element analysis of elliptic problems based on bubble-type local mesh generation. Journal of Computational and Applied Mathematics, 2015, 280, 42-58.	1.1	8
241	A constitutive model for mechanical response characterization of pumpkin peel and flesh tissues under tensile and compressive loadings. Journal of Food Science and Technology, 2015, 52, 4874-4884.	1.4	8
242	Transient air flow and heat transfer due to differential heating on inclined walls and heat source placed on the bottom wall in a partitioned attic shaped space. Energy and Buildings, 2016, 113, 39-50.	3.1	8
243	A Quasi-Conforming Point Interpolation Method (QC-PIM) for Elasticity Problems. International Journal of Computational Methods, 2016, 13, 1650026.	0.8	8
244	An elastic–plastic asperity contact model and its application for micro-contact analysis of gear tooth profiles. International Journal of Mechanics and Materials in Design, 2017, 13, 335-345.	1.7	8
245	A numerical investigation of drug extravasation using a tumour–vasculature microfluidic device. Microfluidics and Nanofluidics, 2018, 22, 1.	1.0	8
246	A 3-D coupled Smoothed Particle Hydrodynamics and Coarse-Grained model to simulate drying mechanisms of small cell aggregates. Applied Mathematical Modelling, 2019, 67, 219-233.	2.2	8
247	Estimation of load conditions and strain distribution for in vivo murine tibia compression loading using experimentally informed finite element models. Journal of Biomechanics, 2021, 115, 110140.	0.9	8
248	GEOMETRICALLY NONLINEAR ANALYSIS OF MICROSWITCHES USING THE LOCAL MESHFREE METHOD. International Journal of Computational Methods, 2008, 05, 513-532.	0.8	7
249	Studies on Bending Limitations for the Optimal Fit of Orthopaedic Bone Plates. Advanced Materials Research, 2012, 602-604, 1181-1185.	0.3	7
250	Prandtl number scaling of the unsteady natural convection boundary layer adjacent to a vertical flat plate for <mml:math <br="" altimg="si2.gif" xmlns:mml="http://www.w3.org/1998/Math/MathML">overflow="scroll"&gt;<mml:mrow><mml:mi mathvariant="italic"&gt;Pr<mml:mo>&gt;</mml:mo><mml:mn>1</mml:mn></mml:mi </mml:mrow></mml:math>	2.5	7
251	subject to ramp surface heat flux. International Journal of Heat and Mass Transfer, 2012, 55, 7046-7055. Unsteady buoyancy driven flows and heat transfer through coupled thermal boundary layers in a partitioned triangular enclosure. International Journal of Heat and Mass Transfer, 2014, 68, 375-382.	2.5	7
252	Unexpected dynamic recrystallization behavior of Ti-7Cu alloy in semi-solid state. Journal of Alloys and Compounds, 2017, 712, 468-476.	2.8	7

#	Article	IF	CITATIONS
253	Uncertainty Quantification in high-density fluid radial-inflow turbines for renewable low-grade temperature cycles. Applied Energy, 2019, 241, 313-330.	5.1	7
254	Multiscale exploit the role of copper on the burn resistant behavior of Ti-Cu alloy. Journal of Alloys and Compounds, 2021, 863, 158639.	2.8	7
255	Deformation of a single red blood cell in a microvessel. ANZIAM Journal, 0, 54, 64.	0.0	7
256	Effective shear modulus approach for two dimensional solids and plate bending problems by meshless point collocation method. Engineering Analysis With Boundary Elements, 2012, 36, 675-684.	2.0	6
257	F-actin crosslinker: A key player for the mechanical stability of filopodial protrusion. Journal of Applied Physics, 2013, 114, 214701.	1.1	6
258	Resonance of graphene nanoribbons doped with nitrogen and boron: a molecular dynamics study. Beilstein Journal of Nanotechnology, 2014, 5, 717-725.	1.5	6
259	Numerical Investigation of Motion and Deformation of a Single Red Blood Cell in a Stenosed Capillary. International Journal of Computational Methods, 2015, 12, 1540003.	0.8	6
260	Tuning the resonance properties of 2D carbon nanotube networks towards a mechanical resonator. Nanotechnology, 2015, 26, 315501.	1.3	6
261	A general approach to tune the vibration properties of the mounting system in the high-speed and heavy-duty engine. JVC/Journal of Vibration and Control, 2016, 22, 247-257.	1.5	6
262	Natural convection subject to sinusoidal thermal forcing on inclined walls and heat source located on bottom wall of an attic-shaped space. Energy and Buildings, 2016, 128, 845-866.	3.1	6
263	Nanojoint Formation between Ceramic Titanate Nanowires and Spot Melting of Metal Nanowires with Electron Beam. ACS Applied Materials & Interfaces, 2017, 9, 9143-9151.	4.0	6
264	Numerical investigation of diesel exhaust particle transport and deposition in the CT-scan based lung airway. AIP Conference Proceedings, 2017, , .	0.3	6
265	Graphynes: an alternative lightweight solution for shock protection. Beilstein Journal of Nanotechnology, 2019, 10, 1588-1595.	1.5	6
266	Two-Dimensional CuTe <sub>2</sub> X (X = Cl, Br, and I): Potential Photocatalysts for Water Splitting under the Visible/Infrared Light. Journal of Physical Chemistry C, 2019, 123, 25543-25548.	1.5	6
267	Application of high-order lattice Boltzmann pseudopotential models. Physical Review E, 2020, 101, 033303.	0.8	6
268	A three-dimensional (3-D) meshfree-based computational model to investigate stress-strain-time relationships of plant cells during drying. PLoS ONE, 2020, 15, e0235712.	1.1	6
269	A data-driven smoothed particle hydrodynamics method for fluids. Engineering Analysis With Boundary Elements, 2021, 132, 12-32.	2.0	6
270	Tensile Performance of Polymer Nanocomposites with Randomly Dispersed Carbon Nanothreads. Macromolecules, 2021, 54, 11486-11496.	2.2	6

#	Article	IF	CITATIONS
271	Stacking-Dependent Interlayer Ferroelectric Coupling and Moiré Domains in a Twisted AgBiP <sub>2</sub> Se <sub>6</sub> Bilayer. Journal of Physical Chemistry Letters, 2022, 13, 2027-2032.	2.1	6
272	Quantitative Fit Assessment of a Precontoured Fracture Fixation Plate: Its Automation and an Investigation on the Borderline Cases. Advanced Materials Research, 2011, 339, 685-689.	0.3	5
273	COLLECTIVE DYNAMICS AND CONTROL OF A 3-D SMALL-WORLD NETWORK WITH TIME DELAYS. International Journal of Bifurcation and Chaos in Applied Sciences and Engineering, 2012, 22, 1250281.	0.7	5
274	A meshfree-based local Galerkin method with condensation of degree of freedom for elastic dynamic analysis. Acta Mechanica Sinica/Lixue Xuebao, 2014, 30, 92-99.	1.5	5
275	MRI magic-angle effect in femorotibial cartilages of the red kangaroo. Magnetic Resonance Imaging, 2017, 43, 66-73.	1.0	5
276	A New Particle Generation Method for Arbitrary 2D Geometries in SPH Modeling. International Journal of Computational Methods, 2017, 14, 1750023.	0.8	5
277	Two- and four-way coupling of cohesive poly-disperse particulate foulants on a metal foam fibre immersed in quiescent fluid. International Communications in Heat and Mass Transfer, 2017, 89, 176-184.	2.9	5
278	A novel numerical model to predict the morphological behavior of magnetic liquid marbles using coarse grained molecular dynamics concepts. Physics of Fluids, 2018, 30, .	1.6	5
279	Atypical Defect Motions in Brittle Layered Sodium Titanate Nanowires. Journal of Physical Chemistry Letters, 2018, 9, 6052-6059.	2.1	5
280	Quantified dense gas conical diffuser performance under uncertainties by flow characteristic analysis. Applied Thermal Engineering, 2019, 161, 114158.	3.0	5
281	How Gaseous Environment Influences a Carbon Nanotube-Based Mechanical Resonator. Journal of Physical Chemistry C, 2019, 123, 25925-25933.	1.5	5
282	Atomic-scale investigation on the ultra-large bending behaviours of layered sodium titanate nanowires. Nanoscale, 2019, 11, 11847-11855.	2.8	5
283	Tumorâ€Targeting Fluorescent Probe Based on 1,8â€Naphthalimide and Porphyrin Groups. ChemistrySelect, 2020, 5, 7680-7684.	0.7	5
284	Carbon Nanotube Reinforced Polyâ€ <i>p</i> â€Phenylene Terephthalamide Fibers for Toughness Improvement: A Molecular Dynamics Study. Advanced Theory and Simulations, 2020, 3, 2000135.	1.3	5
285	Atomistic Mechanisms of Ultralarge Bending Deformation of Single-Crystalline TiO2–B Nanowires. Journal of Physical Chemistry C, 2020, 124, 11174-11182.	1.5	5
286	A point interpolation method for two-dimensional solids. , 2001, 50, 937.		5
287	Two-Dimensional Janus Antimony Selenium Telluride with Large Rashba Spin Splitting and High Electron Mobility. ACS Omega, 2021, 6, 31919-31925.	1.6	5
288	Determination of Elastic Modulus of Thin Coating Materials Using Nanoindentation and Finite Element Analysis. Advanced Materials Research, 0, 76-78, 392-397.	0.3	4

#	Article	IF	CITATIONS
289	A bridging transition technique for the combination of meshfree method with finite element method in 2D solids and structures. Computational Mechanics, 2009, 44, 119-131.	2.2	4
290	Meshless TL and UL Approaches for Large Deformation Analysis. Advanced Materials Research, 0, 139-141, 893-896.	0.3	4
291	A NOVEL QUADRATIC EDGE-BASED SMOOTHED CONFORMING POINT INTERPOLATION METHOD (ES-CPIM) FOR ELASTICITY PROBLEMS. International Journal of Computational Methods, 2012, 09, 1240033.	0.8	4
292	Natural convection from a vertical plate embedded in a stratified medium with uniform heat source. Desalination and Water Treatment, 2012, 44, 7-14.	1.0	4
293	ANALYSIS OF STRAIN-RATE DEPENDENT MECHANICAL BEHAVIOR OF SINGLE CHONDROCYTE: A FINITE ELEMENT STUDY. International Journal of Computational Methods, 2014, 11, 1344005.	0.8	4
294	An effective sub-domain smoothed Galerkin method for free and forced vibration analysis. Meccanica, 2015, 50, 1285-1301.	1.2	4
295	Investigation of the mechanical behavior of kangaroo humeral head cartilage tissue by a porohyperelastic model based on the strain-rate-dependent permeability. Journal of the Mechanical Behavior of Biomedical Materials, 2015, 51, 248-259.	1.5	4
296	Effect of rotating cylinder on heat transfer in a differentially heated rectangular enclosure filled with power law non-Newtonian fluid. International Journal of Numerical Methods for Heat and Fluid Flow, 2016, 26, 1910-1931.	1.6	4
297	A Novel Experimental Method to Assess Particle Deposition in Idealized Porous Channels. Heat Transfer Engineering, 2017, 38, 1008-1017.	1.2	4
298	Thermal Conductivity of Diamond Nanothread. , 2017, , 185-204.		4
299	Stress-Relaxation and Cyclic Behavior of Human Carotid Plaque Tissue. Frontiers in Bioengineering and Biotechnology, 2020, 8, 60.	2.0	4
300	A multiscale modeling method incorporating spatial coupling and temporal coupling into transient simulations of the human airways. International Journal for Numerical Methods in Fluids, 2021, 93, 2905-2920.	0.9	4
301	Tensile properties of functionalized carbon nanothreads. Nano Materials Science, 2022, 4, 220-226.	3.9	4
302	Mechanical Properties of Single‣ayer Diamond Reinforced Poly(vinyl alcohol) Nanocomposites through Atomistic Simulation. Macromolecular Materials and Engineering, 2021, 306, 2100292.	1.7	4
303	Ferroelectric Controlled Gas Adsorption in Doped Graphene/In 2 Se 3 Heterostructure. Advanced Materials Technologies, 0, , 2100463.	3.0	4
304	Tensile Properties of Si Nanowires with Faulted Stacking Layers. Science of Advanced Materials, 2014, 6, 1489-1492.	0.1	4
305	Free convection in a triangular enclosure with fluid-saturated porous medium and internal heat generation. ANZIAM Journal, 0, 52, 127.	0.0	4
306	Deformation characterization of a nanoelectromechanical switch. Journal of Physics: Conference Series, 2006, 34, 118-123.	0.3	3

#	Article	IF	CITATIONS
307	A NODE-BASED SMOOTHED CONFORMING POINT INTERPOLATION METHOD (NS-CPIM) FOR ELASTICITY PROBLEMS. International Journal of Computational Methods, 2011, 08, 801-812.	0.8	3
308	Hardness of silicon nitride thin films characterised by nanoindentation and nanoscratch deconvolution methods. Materials Science and Technology, 2012, 28, 1172-1176.	0.8	3
309	3D CFD Simulations of a Candidate R143A Radial-Inflow Turbine for Geothermal Power Applications. , 2014, , .		3
310	Physical mechanism of the compressive response of F-actin networks: significance of crosslinker unbinding events. Theoretical and Applied Mechanics Letters, 2014, 4, 051006.	1.3	3
311	Anomalous Enhancement of Mechanical Properties in the Ammonia Adsorbed Defective Graphene. Scientific Reports, 2016, 6, 33810.	1.6	3
312	Parametric study on cement treated aggregate panel under impact load. Archives of Civil and Mechanical Engineering, 2018, 18, 622-629.	1.9	3
313	General existence of flexural mode doublets in nanowires targeting vectorial sensing applications. Physical Chemistry Chemical Physics, 2019, 21, 4136-4144.	1.3	3
314	Exceptional Deformability of Wurtzite Zinc Oxide Nanowires with Growth Axial Stacking Faults. Nano Letters, 2021, 21, 4327-4334.	4.5	3
315	Proteoglycan and collagen contribution to the strain-rate-dependent mechanical behaviour of knee and shoulder cartilage. Journal of the Mechanical Behavior of Biomedical Materials, 2021, 124, 104733.	1.5	3
316	Formation of the three-dimensional geometry of the red blood cell membrane. ANZIAM Journal, 0, 54, 80.	0.0	3
317	An Adaptive Local Meshfree Updated Lagrangian Approach for Large Deformation Analysis of Metal Forming. Advanced Materials Research, 2010, 97-101, 2664-2667.	0.3	2
318	Exploration of the Defect's Effect on the Mechanical Properties of Different Orientated Nanowires. Advanced Materials Research, 0, 328-330, 1239-1244.	0.3	2
319	PREDICTION OF STRUCTURAL INTEGRITY, ROBUSTNESS, AND SERVICE LIFE USING ADVANCED FINITE ELEMENT METHODS. International Journal of Computational Methods, 2011, 08, 787-800.	0.8	2
320	A Monte-Carlo simulation method for industry transformer health prediction based on dissolved gas analysis. , 2013, , .		2
321	NUMERICAL SIMULATIONS OF PARTICLE DEPOSITION IN METAL FOAM HEAT EXCHANGERS. International Journal of Computational Materials Science and Engineering, 2013, 02, 1350016.	0.5	2
322	A meshfree-based local Galerkin method with condensation of degree of freedom. Finite Elements in Analysis and Design, 2014, 78, 16-24.	1.7	2
323	Mechano-Ferroelectric Coupling: Stabilization Enhancement and Polarization Switching in Bent AgBiP2Se6 Monolayer. Nanoscale Horizons, 2021, 6, 971-978.	4.1	2
324	Atomistic Insights on the Rheological Property of Polycaprolactone Composites with the Addition of Graphene. Advanced Materials Technologies, 0, , 2100507.	3.0	2

Yuantong Gu

#	Article	IF	CITATIONS
325	The Assessment of Toxicity of Boron Nitride Nanoparticle Using Atomic Forced Microscopy. IFMBE Proceedings, 2015, , 31-34.	0.2	2
326	Natural convection in a triangular enclosure due to non-uniform cooling on top. ANZIAM Journal, 0, 52, 53.	0.0	2
327	A new membrane formulation for modelling the flow of stomatocyte, discocyte, and echinocyte red blood cells. Biomechanics and Modeling in Mechanobiology, 2022, , 1.	1.4	2
328	An effective multiscale approach for deformation analyses of carbon nanotube-based nanoswitches. Proceedings of SPIE, 2008, , .	0.8	1
329	An advanced meshless technique for large deformation analysis of metal forming. Australian Journal of Mechanical Engineering, 2009, 7, 25-32.	1.5	1
330	An Enriched Radial Point Interpolation Method (e-RPIM) for the Analysis of Crack Tip. , 2010, , .		1
331	Influence of pre-exsiting surface defects on the vibrational properties of Ag nanowires. , 2012, , .		1
332	How to Increase the Accuracy of Analysis and Reduce the Computational Time in ANSYS in the Case of Deformation Study of Orthopedic Bone Plates. Advanced Materials Research, 2013, 834-836, 1592-1600.	0.3	1
333	Tensile Properties of Pumpkin Peel and Flesh Tissue and Review of Current Testing Methods. Transactions of the ASABE, 2013, , 1521-1527.	1.1	1
334	A stochastic thermostat algorithm for coarse-grained thermomechanical modeling of large-scale soft matters: Theory and application to microfilaments. Journal of Computational Physics, 2014, 263, 177-184.	1.9	1
335	Comprehensive Contribution of Filament Thickness and Crosslinker Failure to the Rheological Property of F-actin Cytoskeleton. Cellular and Molecular Bioengineering, 2015, 8, 278-284.	1.0	1
336	Physical mechanisms underlying the strain-rate-dependent mechanical behavior of kangaroo shoulder cartilage. Applied Physics Letters, 2015, 107, 103701.	1.5	1
337	Prediction of atherosclerotic plaque life – Perceptions from fatigue analysis. Procedia Manufacturing, 2019, 30, 522-529.	1.9	1
338	Smoothed Finite Element Methods for Predicting the Mid to High Frequency Acoustic Response in the Cylinder-Head Chamber of a Diesel Engine. International Journal of Computational Methods, 2020, 17, 1950060.	0.8	1
339	Atomic Investigation on the Facetâ€Dependent Melting of Ceramic Nanostructures via In Situ Electron Irradiation. Advanced Materials Interfaces, 2020, 7, 2000288.	1.9	1
340	Effect of Fe-doping on bending elastic properties of single-crystalline rutile TiO2 nanowires. Nanoscale Advances, 2020, 2, 2800-2807.	2.2	1
341	Revealing the Mechanical Bending Mechanisms of Single-Crystalline Rutile TiO <sub>2</sub> Nanowires Near Room Temperature: Implications for Nanostructured Semiconductors. ACS Applied Nano Materials, 2021, 4, 10354-10359.	2.4	1
342	Numerical Study of the Flow Behaviour of Discocyte Red Blood Cell Through a Non-uniform Capillary. , 2020, , .		1

#	Article	IF	CITATIONS
343	Modelling 3-D cellular microfluidics of different plant cells for the prediction of cellular deformations under external mechanical compression: A SPH-CG-based computational study. , 2020, , .		1
344	Particle-Based Numerical Modelling of Liquid Marbles: Recent Advances and Future Perspectives. Archives of Computational Methods in Engineering, 2022, 29, 3021-3039.	6.0	1
345	Molecular basis of transport of surface functionalised gold nanoparticles to pulmonary surfactant. RSC Advances, 2022, 12, 18012-18021.	1.7	1
346	A STUDY ON THE PATCH TEST OF POINT INTERPOLATION METHODS. , 2002, , .		0
347	A HYBRID BOUNDARY POINT INTERPOLATION METHOD (HBPIM) AND ITS COUPLING WITH EFG METHOD. , 2002, , .		0
348	STRESS ANALYSIS OF 3-D SOLIDS USING A MESHFREE RADIAL POINT INTERPOLATION METHOD. , 2006, , 1555-1559.		0
349	A coupled numerical approach for nonlinear dynamic fluidâ€structure interaction analysis of a nearâ€bed submarine pipeline. Engineering Computations, 2008, 25, 569-588.	0.7	0
350	A Coupled Meshless Techniqueâ^•Molecular Dynamics Approach for Deformation Characterization of Mono-crystalline Metal. , 2010, , .		0
351	Theoretical Analysis of Serrated Chip Formation Based on Ideal Models in High Speed Cutting. Advanced Materials Research, 0, 154-155, 239-245.	0.3	0
352	A Modified Quality Control Method for Manufacturing Process in Mask Industry. Advanced Materials Research, 0, 139-141, 1843-1846.	0.3	0
353	Survival analysis using neural network hazard model with incomplete covariate data. , 2011, , .		0
354	A nanoscratch method for measuring hardness of thin films. International Journal of Nanomanufacturing, 2011, 7, 427.	0.3	0
355	Effect of Micro Scale on Prediction of Thermal Residual Stresses in Multilayer Ceramic Capacitors (MLCCs). Advanced Materials Research, 2011, 295-297, 2651-2654.	0.3	0
356	Mixed Convection Over a Horizontal Plate With Streamwise Non-Uniform Surface Temperature Distribution. Journal of Heat Transfer, 2013, 135, .	1.2	0
357	An agent-based method for simulating porous fluid-saturated structures with indistinguishable components. Physica A: Statistical Mechanics and Its Applications, 2017, 483, 36-43.	1.2	0
358	Heat Transfer Enhancement in a Baffled Attic-Shaped Space. Green Energy and Technology, 2018, , 157-172.	0.4	0
359	Optimizing the Unrestricted Wind Turbine Placements with Different Turbine Hub Heights. Lecture Notes in Mechanical Engineering, 2018, , 263-275.	0.3	0
360	A CONFORMING POINT INTERPOLATION METHOD FOR ANALYZING SPATIAL THICK SHELL STRUCTURES. , 2002, , .		0

#	Article	IF	CITATIONS
361	AN APPROACH FOR NODAL SELECTION IN MFREE2D <sup><math>\hat{A}</math>©</sup> ., 2002, , .		0
362	AN ELASTO-PLASTIC ANALYSIS OF SOLIDS BY THE LOCAL MESHLESS METHOD BASED ON MLS. , 2009, , .		0
363	Atomistic Investigations of Single-Crystal Silicon with Pre-Existing Defects. Advanced Science Letters, 2012, 14, 165-170.	0.2	Ο
364	Prandtl number scaling of natural convection of an inclined flat plate due to uniform surface heat flux. ANZIAM Journal, 0, 53, 387.	0.0	0
365	Numerical Characterization of Nanowires. , 2013, , .		Ο
366	Hyperelastic Constitutive Relationship for the Strain-Rate Dependent Behavior of Shoulder and Other Joint Cartilages. IFMBE Proceedings, 2014, , 255-258.	0.2	0
367	Molecular Sliding Filament Model for Muscular Contraction Based on Multiscale Investigation. Science of Advanced Materials, 2014, 6, 1346-1350.	0.1	Ο
368	10.1063/1.5079438.1.,2019,,.		0
369	Ferroelectric Controlled Gas Adsorption in Doped Graphene/In <sub>2</sub> Se <sub>3</sub> Heterostructure (Adv. Mater. Technol. 4/2022). Advanced Materials Technologies, 2022, 7, .	3.0	0